In vitro elucidation of the therapeutic applications of biosynthesized selenium nanoparticles using *Saussurea costus* root extract

Manal Almughamisi

Department of Clinical Nutrition, College of Applied Medical Sciences, Taibah University, Saudi Arabia

Corresponding Author: Manal Almughamisi, Department of Clinical Nutrition, College of Applied Medical Sciences, Taibah University, Saudi Arabia. Email: mmughamisi@taibahu.edu.sa

Academic Editor: Ismail Eş, PhD, Institute of Biomedical Engineering, Old Road Campus Research Building, University of Oxford, Headington, Oxford OX3 7DQ, UK

Received: 24 March 2025; Accepted: 30 September 2025; Published: 18 November 2025
© 2025 Codon Publications

OPEN ACCESS

RESEARCH ARTICLE

Abstract

Saussurea costus contains a variety of bioactive chemicals vital for biomedical use. The unique benefits of selenium nanoparticles (SeNPs) make them very desirable in various sectors. The emergence of green techniques employing ecological assets is a result of growing need for sustainable and environment-friendly nanomaterial synthesis. The aim of this investigation is to create green SeNPs by using root extract of *S. costus* and evaluate the therapeutic benefits of the generated SeNPs with those of *S. costus* extract. *S. costus* was processed with 90% ethanol, and analyzed by high-performance liquid chromatography. The biosynthesized nanomaterials were examined. In all, 15 compounds were detected in the extract, where rutin, chlorogenic acid, and coumaric acid were the most common molecules determined. The produced SeNPs had a characteristic peak at 275 nm, with a mean size of 73.7±0.7 nm. There is a characteristic pattern for SeNPs that could be observed through Fourier-transform infrared spectroscopy and X-ray diffraction analysis. SeNPs were found to have better anti-*Helicobacter pylori* impact than *S. costus* extract. The produced nanocrystals had an inhibition diameter of 30.7±0.2 mm and a minimum inhibitory concentration of 15.62±0.2 µg/mL. Also, 2,2-diphenyl-1-picrylhydrazyl (DPPH) testing showed that SeNPs had a half-maximal inhibitory concentration (IC_{50}) = 9.42±0.1 µg/mL. Furthermore, the prepared nanoparticles had a promising anti-inflammatory impact with IC_{50} = 8.33±0.4 µg/mL. The biosynthesized nanoparticles had a better alpha glucosidase level and alpha amylase level than *S. costus* extract. SeNPs showed promising anticancer activity against human epithelial cell line Caco-2 (a cell line originally derived from colon carcinoma). This was confirmed by analyzing cell cycle changes using flow cytometry. Collectively, SeNPs prepared from *S. costus* had *in vitro* multi-therapeutic functions to be used in the future pharmaceutical applications.

Keywords: Saussurea costus; selenium nanoparticles; *H. pylori;* antidiabetic*;* anticancer; cell cycle

Introduction

Traditional medicine has utilized herbs and their extracts since ancient times. Because it includes natural medicinal components, over 80% of people still rely on herbal therapy. Examples include, but are not limited to, medicinal substances that can reduce the growth of various cancer cell types and impede the proliferation of various pathogenic microorganisms (Azmir *et al*., 2013; Tsiaka *et al*., 2017). Herbal extracts also have antioxidant properties, which are crucial for lowering oxidative stress (Elshaer *et al*., 2022). In addition to the medical sector, the fields of dietary intake, nutritional supplements, and cosmetics also use herbs and their extracts (Ahmed *et al*., 2022). Almost 85,000 species of plants for used for medicinal purposes globally. However, many of these species with many phytochemicals are still unexplored; *Sausurea costus* (*S. costus*), belonging to the Asteraceae

ISSN 1757-837X online, DOI 10.15586/qas.v17i4.1591

family, is one of these unexplored pharmaceutical plants (Elshaer *et al.*, 2024).

Saussurea costus, a plant of medicinal importance, has been used for long in conventional Saudi Arabian medicine. Being a threatened species, it is thoroughly studied for its chemical formula, importance, and therapeutic value for conventional phytomedicine. It exhibits a variety of biological activities (Elnour and Abdurahman, 2024; Mujammami, 2020).

The goal of nanotechnology is to create nanoparticles (NPs) with controlled dimensions, form, and chemical makeup that could be used for the health benefits of humans. Although some of the physical and chemical methods (e.g., ball milling, chemical vapor deposition) can successfully manufacture well-defined nanoparticles, they are expensive and may present environmental hazards (Bhattacharya and Rajinder, 2005; Sastry *et al.*, 2004). Nanoparticles are produced using a variety of methods, the most popular of which are chemical ones (Mohanpuria *et al.*, 2008). Green synthesis methods provide a viable option by producing nanoparticles from sustainable resources, such as bio-based substances (Almayouf *et al.*, 2024; Karim *et al.*, 2023; Xu *et al.*, 2023).

The possible use of metal nanoparticles as antibacterial substances has generated a lot of interest (Alshahrani *et al.*, 2021; Rezaei *et al.*, 2021). The high biocompatibility and low cytotoxicity of selenium nanoparticles (SeNPs) have made them popular and are widely used in food science and pharmaceuticals (Pon Matheswari *et al.*, 2022). High absorption, low toxicity, and strong antibacterial and antioxidant activity are reported for SeNPs (Mellinas *et al.*, 2019). A viable substitute for physical and chemical methods for the synthesis of SeNPs is the incorporation of microbes, plant extracts, and green chemistry (Adibian *et al.*, 2022). There are a number of benefits for using biological or environment-friendly methods to produce inorganic nanoparticles. For example, biosynthetic methods are low-cost, environmentally benign, one-step, and clean processes that reduce or completely eradicate pollutants and ecological harm (Esmaili *et al.*, 2022). Through the provision of reducing/stabilizing agents and herbal capping, plant extract-mediated nanoparticles enhance the formation of SeNPs. Furthermore, the formation of SeNPs can be accelerated in a single step by the bioactive ingredients present in plant extracts (Korde *et al.*, 2020; Shayan *et al.*, 2024). There is a great need to apply green synthesized nanoparticles in many medical applications. *S. costus* is used to prepare many nanoparticles, but few studies are conducted to prepare SeNPs and test its variable applications (Ao *et al.*, 2023). There is a recent trend to investigate the various possible biological activities of plant extract-mediated nanoparticles. The objective of the current work was to biosynthesize SeNPs from the root extract of *S. costus*, characterization of the prepared nanoparticles, and comparing some of the *in vitro* biological activities of prepared extract and green synthesized SeNPs.

Materials and Methods

Plant and chemicals

The chemicals used in the study were acquired from Sigma Co. Ltd. (St. Louis, MO, USA). Fresh roots of *S. costus* were acquired from a local specialty herbal shop in Saudi Arabia. The identification of roots was confirmed at Al-Azhar University's Faculty of Science in Cairo, Egypt with reference No. AZH-E-226. The sample's certificate of authenticity was recorded at the faculty's public herbarium.

Preparation of *S. costus* extract

In all, 50 g of dry roots of *S. costus* were homogenized, kept in a secured vessel, and mixed with 0.5 L of 90% ethanol. The mixed contents were left for 3 days in glass jars at an ambient temperature. The extract was kept for 60 min in a disruptor that was set at 40°C for traditional extraction method. After filtration and spinning the extract in a rotatory evaporator at 40°C, crude extract was created (Marinova *et al.*, 2005).

High-performance liquid chromatography (HPLC) examination of *S. costus* extract

A 10 µL aliquot of the *S. costus* extract was injected into the HPLC system (Agilent Technologies, CA, USA) equipped with a C18 column (4.7 mm × 250 mm, 10 µm particle size). The column temperature was maintained at 46 °C. The mobile phase consisted of (a) water and (b) acetic acid (0.05%) in acetonitrile at a flowing rate of 0.99 mL per minute. The mobile phase was set up as follows: 0 (82% A), 0–1 (85% A), 1–11 (70% A), 11–18 (65% A), 18–22 (80% A), and 22–24 (80% A). Additionally, the multi-wavelength detector was recorded at 280 nm. An injection volume of 5.0 µL was used for every sample solution (Gupta *et al.*, 2023).

Preparation of SeNPs using *S. costus* extract

In all, 80-µL aliquot of *S. costus* extract (50 mg/mL) was incorporated into Na_2SeO_3 solution at the final level of 10 mM in order to synthesize SeNPs. The biosynthesis process was performed by continuous stirring at 1,400 rpm for 35 min at 42°C. The reaction was completed at an

ambient temperature in 24 h with continuous stirring in the dark. The solution with colloidal particles was kept for further examination and use at 5°C (Garza-García *et al.*, 2023).

Characterization of SeNPs

The produced SeNPs were analyzed at 200–600 nm using a UV spectrophotometer (Drawell, China). The field emission scanning electron microscope (SEM; JEOL, Japan) was used to investigate the produced particles. Energy dispersing X-ray (EdX) was used to analyze various percentages of elements in the prepared SeNPs. Besides, SeNPs and *S. costus* extract spectra were produced and the functional groups were examined at a range of 400–4,000 cm^{-1} using Fourier-transform infrared spectroscopy (FTIR; L160001J, PerkinElmer, USA). Additionally, X-ray diffraction (XRD) structures of SeNPs at a potential of 40 kV and an output current of 30 mA, together with an inversely opposite Ni-filter Cu-Kk energy, were used to assess the crystallographic features of the resulting SeNPs (Soliman *et al.*, 2024).

Detection of anti-*Helicobacter pylori* activity and determination of minimal inhibitory concentration (MIC) and minimal bactericidal concentration (MBC)

To evaluate the effects of the produced SeNPs and the *S. costus* extract on *Helicobacter pylori*, a standard *H. pylori* strain was cultured and used for antimicrobial testing (ATCC 43504) was provided by the Microbiology Department of Assuit University, Assiut, Egypt.

The anti-*H. pylori* properties were tested *in vitro* through the well agar diffusion method. In brief, Mueller–Hinton agar plates supplemented with 10% sheep blood were inoculated with 100 µL of *Helicobacter pylori* suspension (1.0×10^8 CFU/mL). Wells of 6 mm diameter were then aseptically created in the agar using a sterile cork borer. Subsequently, 100 µL of each test sample (the *S. costus* extract or SeNPs) was added to the respective wells to evaluate antibacterial activity. Dimethyl sulfoxide (DMSO) was used as a negative control, while the antibiotics amoxicillin (0.06 mg/mL) and clarithromycin (0.06 mg/mL) were used as positive controls. The inhibition area's dimensions were measured after 72-h incubation at 35°C in a moist microaerophilic device (Santiago *et al.*, 2022).

For minimal inhibitory levels: Using nutritious broth for bacteria, the micro-dilution broth technique was used to determine the samples' MIC. Each of the samples under investigation was diluted for two times to determine ultimate levels, which varied between 0.98 µg/mL and 1,000 µg/mL. To prepare 96-well microtitrate plate, 200 µL of the sample dilution under investigation in broth medium was placed in each well. The inoculum was generated using fresh bacterial cultures that satisfied the turbidity requirements of the 1.0 McFarland standard. To reach a level of 3.0×10^6 CFU/mL, 2.0 µL of sterilized 0.9% NaCl was added to each well. After that, the bacteria were cultured at 35°C for 72 h. Concentrations of the items at which development of the standard strain was totally inhibited were visibly measured to determine MICs. Positive control (inoculum containing the subjected samples) and a negative reference (estimated samples containing no inoculum) were present on each microplate (Huang *et al.*, 2021).

To determine the minimal bactericidal concentration (MBC), 100 µL from each well that showed complete inhibition of bacterial growth in the MIC assay was subcultured onto Mueller–Hinton agar plates supplemented with 10% sheep blood. The plates were then incubated at 35 °C for 72 hours. The MBC was defined as the lowest concentration of the sample that produced no visible bacterial colonies after incubation. The MBC–MIC ratios were calculated to determine whether the bactericidal or bacteriostatic activity of the investigated substance inhibited the microbial growth (Huang *et al.*, 2021).

Assessment of antioxidant activity

To determine the antioxidant activity of the examined specimens, 0.10 mM *2,2-diphenyl-1-picrylhydrazyl* (DPPH)-containing ethanol solution was utilized. Different concentrations of the samples in ethanol (ranging from 3.9 µg/mL to 1,000 µg/mL) were mixed with 3 mL of the prepared reagent solution. The mixtures were thoroughly shaken and left to stand for 30 minutes at room temperature to allow color development. The absorbance of each sample was then measured at 520 nm using a UV–Vis spectrophotometer to determine the antioxidant activity (Gueffai *et al.*, 2022).

Elucidation of anti-inflammatory activity

To ascertain the anti-inflammatory capabilities of both specimens, membrane stabilization testing was performed. A range of sample concentrations, from 100 to 1,000 µg/mL, was created. The acquired samples were infused with hypotonic liquid. As negative and positive standards, indomethacin and purified water were used, respectively. Following the addition of 500 µL of samples to new erythrocyte suspension (3.0%) in 0.8 mL of saline, the mixture was incubated for 2 h at 35°C. At 7°C, the mixture was spun for 20 min at 14,000 ×g. Sample absorption was measured at 580 nm (Amina *et al.*, 2023).

Determination of antidiabetic impact

Alpha-glucosidase testing

The α-glucosidase activity of specimens was measured. For 30 min at 30°C, 50-µL samples containing various amounts (1.97–1,000 µg/mL) were maintained with 10.0 µL of α-glucosidase enzyme solution (1.0 U/mL) and 125.0 µL of 0.12-M phosphate buffer (pH 7.3). To start the reaction after 20 minutes, 20 µL of 1-M pNPG (substrate) was added and the mixture was allowed to stand for 35 min. The reaction was stopped with the addition of 50 µL of 0.1-N Na_2CO_3, and absorption at 415 nm was measured using a spectrophotometer (Biosystm 310 plus, USA) (Taher *et al.*, 2016).

Alpha amylase assay

The test was conducted using the 3,5-dinitrosalicylic acid (DSNA) technique. To get values ranging from 1.9 to 1,000 µg/mL, the extract was initially dispersed in 10% DMSO and then in buffer (0.020-M NaH_2PO_4/ NaH_2PO_4 and 0.0090-M NaCl at pH 7.3). In total, 200 µL of each sample was mixed with 2.0 units/mL of α-amylase solution, and the mixture was incubated at 35 °C for 12 minutes

After that, each tube received 200 µL of 1.0% starch in water (w/v) solution, and the tubes were allowed to stand for 3 min. A water bath was used to heat the mixture for 12 min at 70°C after adding 200 µL of DNSA reagent (12.0 g of sodium potassium tartrate tetrahydrate in 8.0 mL of 2-M sodium hydroxide and 20 mL of 96-mM 3,5-dinitrosalicylic acid solution) to stop the reaction. Once the mixture had reached ambient temperature, it was diluted with 5 mL of deionized water and its absorption at 580 nm was measured using a UV-visible (Biosystem 310, USA) spectrophotometer (Oboh *et al.*, 2012).

Cytotoxicity by MTT testing

The MTT (3-(4,5-dimethylthiazol-2-yl)-2,5-diphenyltetrazolium bromide) assay was conducted to investigate the cytopathic influence on human epithelial Caco-2 cell line as cancer cells (a cell line originally derived from colon carcinoma) and Wi-38 as normal cells for the prepared samples after it became dispersed in DMSO. The result was a blue color that was directly proportional to the quantity of the living cells when evaluated with conventional phases. Absorbance was measured at 560 nm by utilizing a computerized microplate analyzer (BMG, LabTech, Australia). After the cells were allowed to adhere and form a confluent monolayer for 24 h, samples containing 1,000–31.25 µg/mL were added, and the cells were subsequently incubated for another 24 h at 35°C. MTT solution, 100 µL (5.0 mg/mL), was incorporated along with the fresh media, and it was kept at 35°C for 4 h. A CCD camera and a microscope (Accu-Scope INC., USA) were used to view the cells (Alsanosi *et al.*, 2022).

Flow cytometry analysis of cell cycle

Using flow cytometry, the impact of SeNPs on Caco-2 cells' cell cycle phase was investigated. Prior to being subjected to the SeNP's half-maximal inhibitory concentration (IC_{50}), Caco-2 cells were first cultivated for 24 h at a density of 1.6×10^6 cells/mL in a tissue culture plastic plate. Following trypsinization, the cells were washed with phosphate-buffered saline (PBS) and fixed at -20°C with ice-cold 70% ethanol. After that, the cells were treated with propidium iodide (PI) solution (Cytoflex Beckman, Germany) for 30 min at 5°C. The cell cycle phases were investigated by using flow cytometry (Cytexpert Software, Germany) (Cháirez-Ramírez *et al.*, 2021).

Statistics for the results

The results were displayed as mean±SD values for each experiment, which was conducted for three times. With the Graph Pad Prism V5 (San Diego, CA, USA) software, *t*-test was used to analyze disparity in mean values. Significant variation was defined as results with $P < 0.05$.

Results

Determination of various bioactive compounds in *S. costus* extract

Different phenolic and flavonoids were observed as bioactive molecules in the ethanol extract of *S. costus* roots upon separation by HPLC (Supplementary Figure S1 and Table 1). In all, 15 compounds were detected in the *S. costus* extract, with seven major compounds, which were rutin, chlorogenic acid, coumaric acid, gallic acid, coffeic acid, naringenin, and syringic acid. Eight compounds present in low levels were daidzein, rosmarinic acid, ferulic acid, quercetin, cinnamic acid, methyl gallate, kaempferol, and hesperetin (Table 1).

Examination of biosynthesized SeNPs

A distinctive peak for the prepared SeNPs was observed at 275 nm upon screening using UV spectrophotometer (Figure 1A). Besides, transmission electron microscopic (TEM) analysis revealed the structure of prepared nanoparticles with a mean size of 73.7±0.7 nm (see Figure 1B). Furthermore, EdX analysis showed various proportions of elements in the prepared form, with selenium having a percentage of 23.7% as illustrated in

Table 1. Different polyphenolic compounds and flavonoids in ethanol root extract of *S. costus* (dilution 1:10) separated using HPLC.

No.	Ret. time(min)	Compound name	Area (%)
1.	3.559	Gallic acid	6.642
2.	4.244	Chlorogenic acid	17.054
3.	5.315	Methyl gallate	0.133
4.	5.872	Coffeic acid	5.193
5.	6.416	Syringic acid	1.405
6.	7.114	Rutin	46.532
7.	8.713	Coumaric acid	15.642
8.	9.682	Ferulic acid	0.921
9.	10.382	Naringenin	4.173
10.	11.759	Rosmarinic acid	0.566
11.	16.014	Daidzein	0.982
12.	17.737	Querectin	0.317
13.	19.397	Cinnamic acid	0.253
14.	20.851	Kaempferol	0.111
15.	21.437	Hesperetin	0.070

Figure 1C. FTIR analysis of *S. costus* extract was performed and compared with the peaks of SeNPs. A characteristic peak at 3,389 cm^{-1} was observed in *S. costus* extract that become shaper in SeNPs at 3,419 cm^{-1} for O-H stretching vibrations, 1,418 cm^{-1} for COO-group, and 719 cm^{-1} for C-H stretching vibrations. A peak at 462 cm^{-1} for the SeNP pattern showed the existence of selenium in nano-solution, which revealed production by *S. costus* extract as depicted in Figure 2A. XRD testing at a range of 10°–80° showed various characterized peaks as observed at angles of 100°, 101°, 111°, 201°, 210°, and 213°, and followed the Miller indices as shown in Figure 2B.

Anti-*H. pylori* for *S. costus* extract and SeNPs, MICs, and MBCs

Both *S. costus* extract and prepared SeNPs were tested for *H. pylori* as shown in Figure S2. It was observed that SeNPs had the highest inhibition zone of 30.7±0.2 mm,

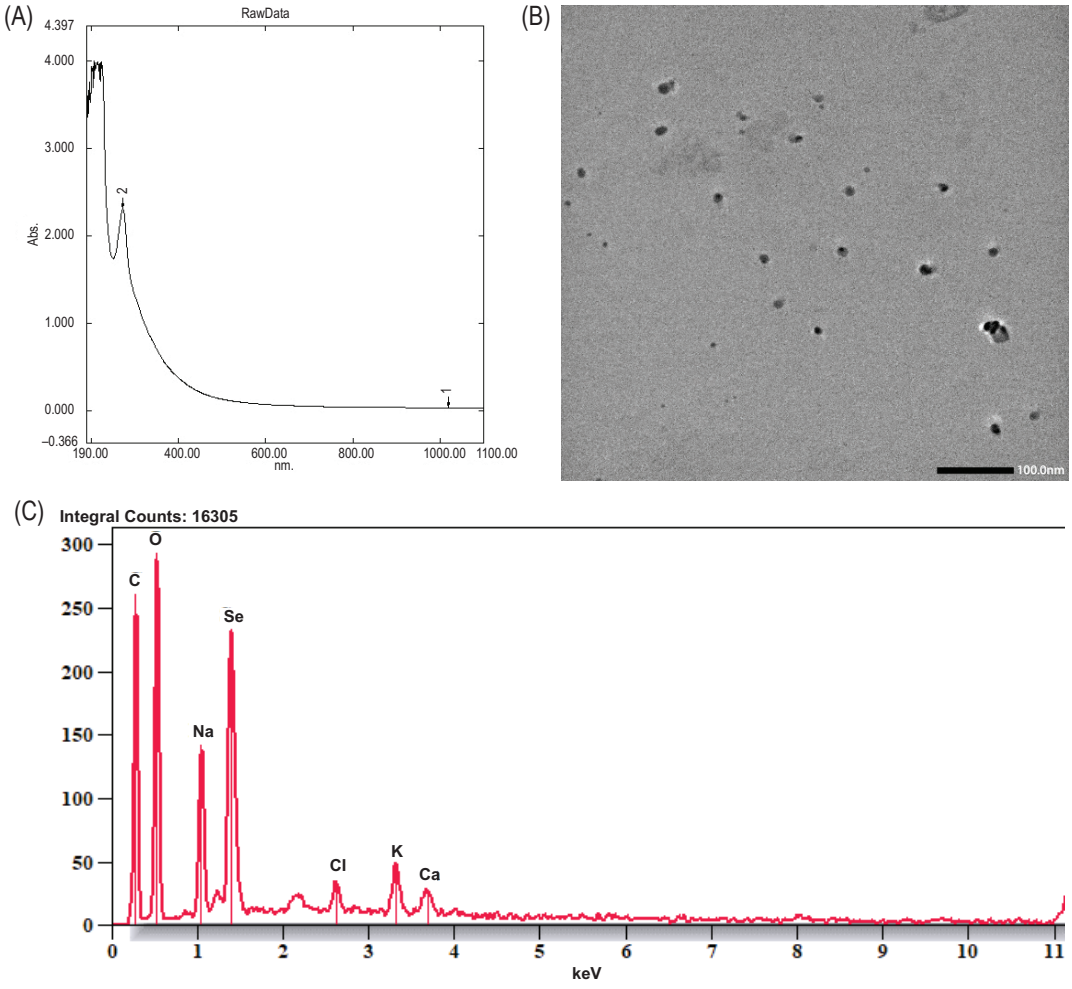

	C	O	Na	Cl	K	Ca	Se
SeNPs sample	30.4	35.2	7.3	0.9	1.5	1.0	23.7

Figure 1. 1C shows the EDX spectrum and elemental composition of the biosynthesized SeNPs, indicating the presence of selenium (23.7 wt%), carbon (30.4 wt%), oxygen (35.2 wt%), and trace amounts of sodium, chlorine, potassium, and calcium."

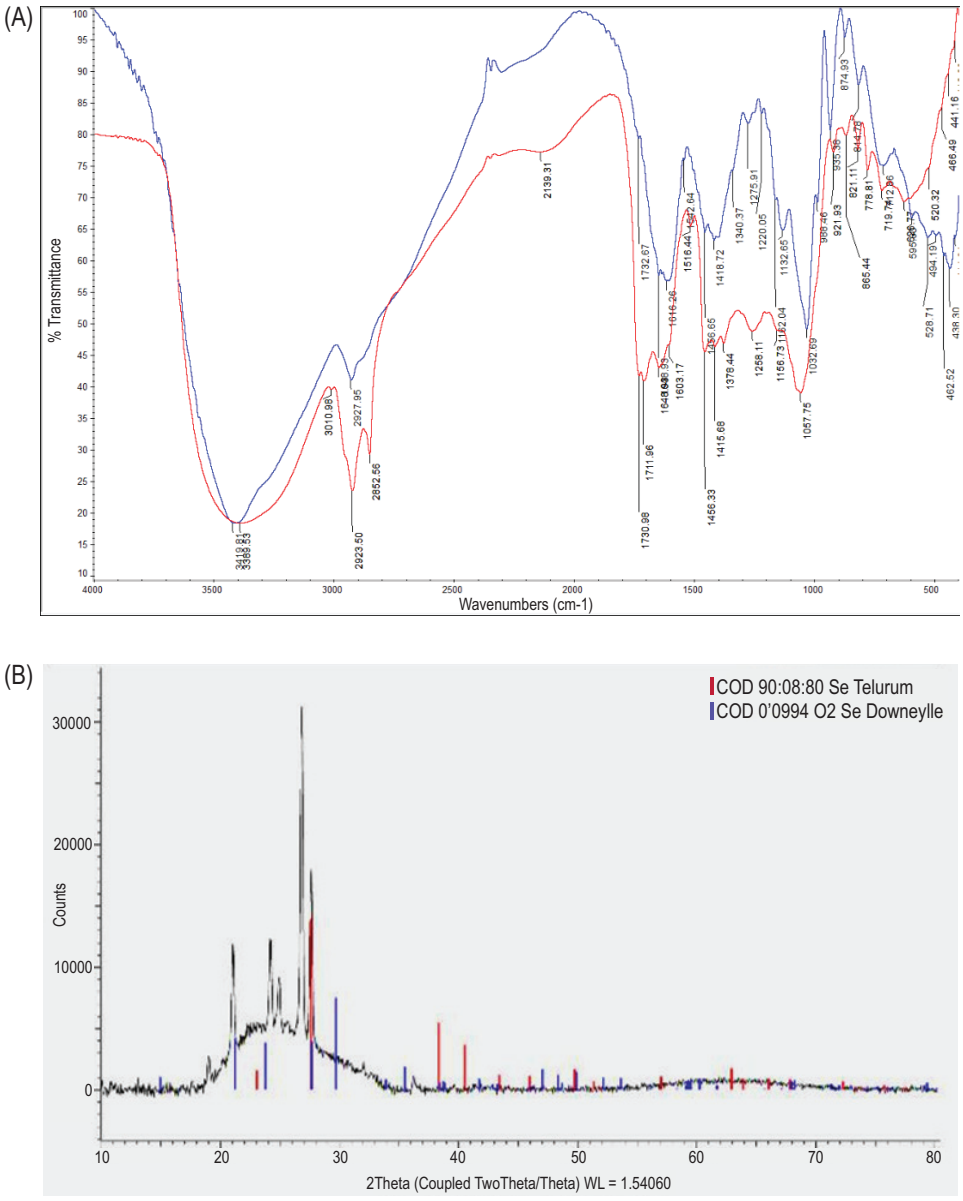

Figure 2. Characterization of prepared SeNPs. (A) FTIR for overlay of *S. costus* extract (red line) and SeNPs (blue line); (B) XRD pattern of SeNPs.

while the inhibition zones for *S. costus* extract and the control drug were 27.3±0.2 mm and 23.7 ±0.2 mm, respectively, as illustrated in Table 2. The MIC and MBC determined for SeNPs was 15.62±0.2 µg/mL, while the MICs and MBCs for *S. costus* extract and the control drug were 31.25±0.1 µg/mL and 62.5±0.1 µg/mL, respectively, as shown in Table 2.

Table 2. Anti-*H. pylori* impact, MICs, and MBCs of *S. costus* extract and the prepared SeNPs, compared to the control.

Sample	Inhibition zone (mm)		
S. costus extract	27.3±0.2		
SeNPs	30.7±0.2		
Control	23.7±0.2		
Sample	**MIC (µg/mL)**	**MBC (µg/mL)**	**MBC/MIC index***
S. costus extract	31.25±0.1	62.5±0.1	2
SeNPs	15.62±0.2	15.62±0.2	1
Control	31.25±0.1	62.5±0.1	2

Notes: Results are recorded as mean±SD values.
*The MBC/MIC values of the samples ≤4 represent their bactericidal activity versus H. pylori, while the MBC/MIC values of the samples >4 represent their bacteriostatic functions.

omparing of antioxidant activity of *S. costus* extract and SeNPs

The DPPH scavenging activity of the produced SeNPs was 9.42±0.1 µg/mL, while the DPPH scavenging activity of *S. costus* extract was 18.0±0.2 µg/mL. In addition,

the antioxidant value of ascorbic acid (control) was 2.36±0.2 µg/mL. There was a significant difference between *S. costus* extract, SeNPs, and the control ($P \leq 0.05$) as depicted in Figure 3.

Comparative assessment of anti-inflammatory effect of *S. costus* extract and SeNPs

The anti-inflammatory activity of the synthesized SeNPs was 8.33 ±0.4 µg/mL, while the anti-inflammatory activity of *S. costus* extract was 16.46 ±0.3 µg/mL. In addition, the anti-inflammatory value of diclofenac as a control was 6.05±0.2 µg/mL. There was a striking difference between *S. costus* extract, SeNPs, and the control ($P \leq 0.05$), as depicted in Figure 4.

Comparative assessment of antidiabetic activity for *S. costus* extract and SeNPs

The evaluation of alpha-glucosidase enzyme level in *S. costus* extract reveled its IC_{50} = 23.63±0.6 µg/mL, while for the alpha-glucosidase enzyme level in SeNPs, IC_{50} = 12.55±0.8 µg/mL. On the other hand, for level for the control, IC_{50} = 6.27±0.4 µg/mL. There was a significant difference between *S. costus* extract, SeNPs, and the control ($P \leq 0.05$), as shown in Figure 5A.

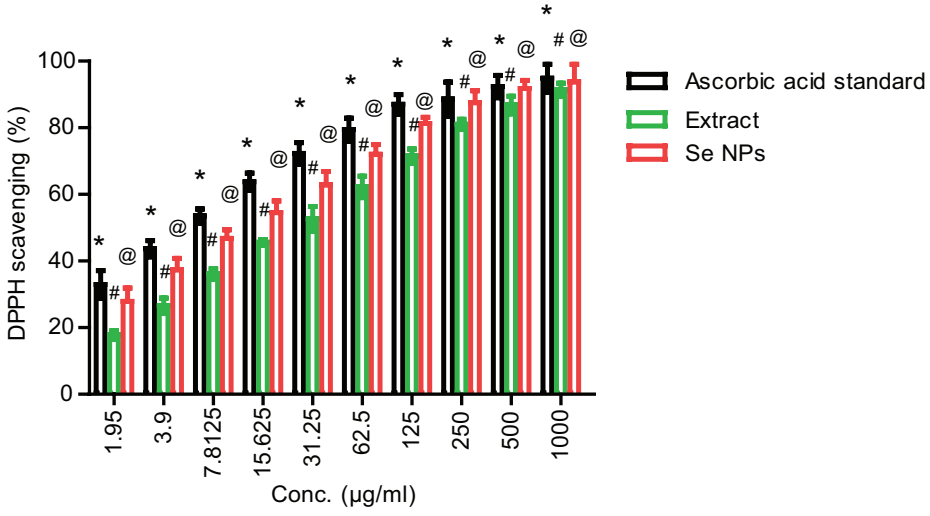

Figure 3. Antioxidant activity of *S. costus* roots extract and SeNPs, compared to ascorbic acid as a control (data are recoded as mean±SD values; different symbols refer to significant difference at P ≤ 0.05).

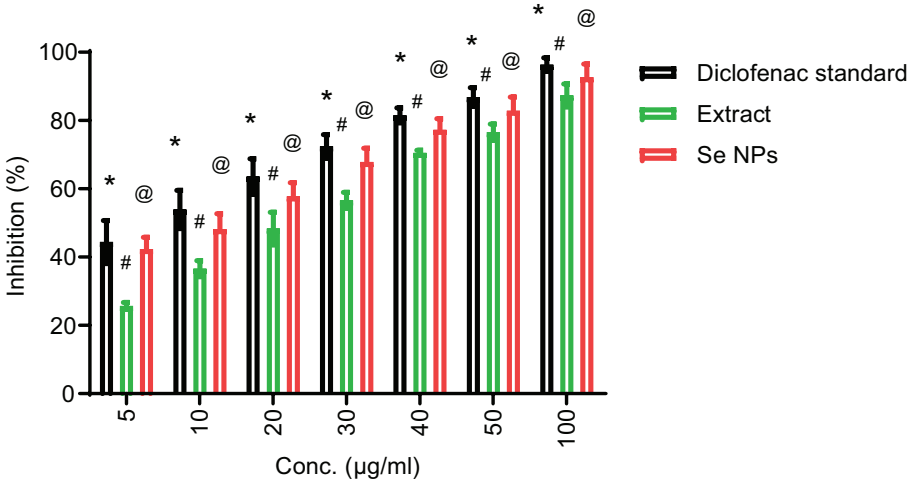

Figure 4. Anti-inflammatory activity of *S. costus* roots extract and SeNPs, compared to the control (data are represented as mean±SD values; various symbols refer to significant variations at P ≤ 0.05).

Determination of the level of alpha-amylase enzyme in *S. costus* extract showed its IC_{50} =21.18±0.2 µg/mL. On the other, SeNPs showed a promising alpha-amylase activity with IC_{50} = 8.75±0.3 µg/mL, whereas the level for the control was detected at IC_{50} = 4.51±0.4 µg/mL. These results revealed a significant variation between two treatments and the control, as illustrated in Figure 5B.

Assessment of cytopathic impact of *S. costus* extract and SeNPs

The *S. costus* extract showed a promising anticancer effect toward Caco-2 cells with IC_{50} = 82.77±1.02 µg/mL. There is a significant rise ($P \leq 0.05$) in anticancer effect toward Caco-2 cells upon using the prepared SeNPs with IC_{50} = 34.09±2.49 µg/mL, as shown in Figure 6 and Supplementary Table S1. On the other hand, both *S. costus* extract and biosynthesized SeNPs had a minimal cytotoxic activity toward Wi-38 cells with IC_{50} = 146.5±0.52 and 87.91±0.45 µg/mL, respectively, as depicted in Figure 7 and Supplementary Table S2.

Comparative assessment of cell cycles

There was a dramatic reduction ($P \leq 0.05$) in percentage in the G0 phase (resting phase) of Caco-2 cells upon treatment with *S. costus* extract and SeNPs, while a non-significant difference was observed in the proportions of

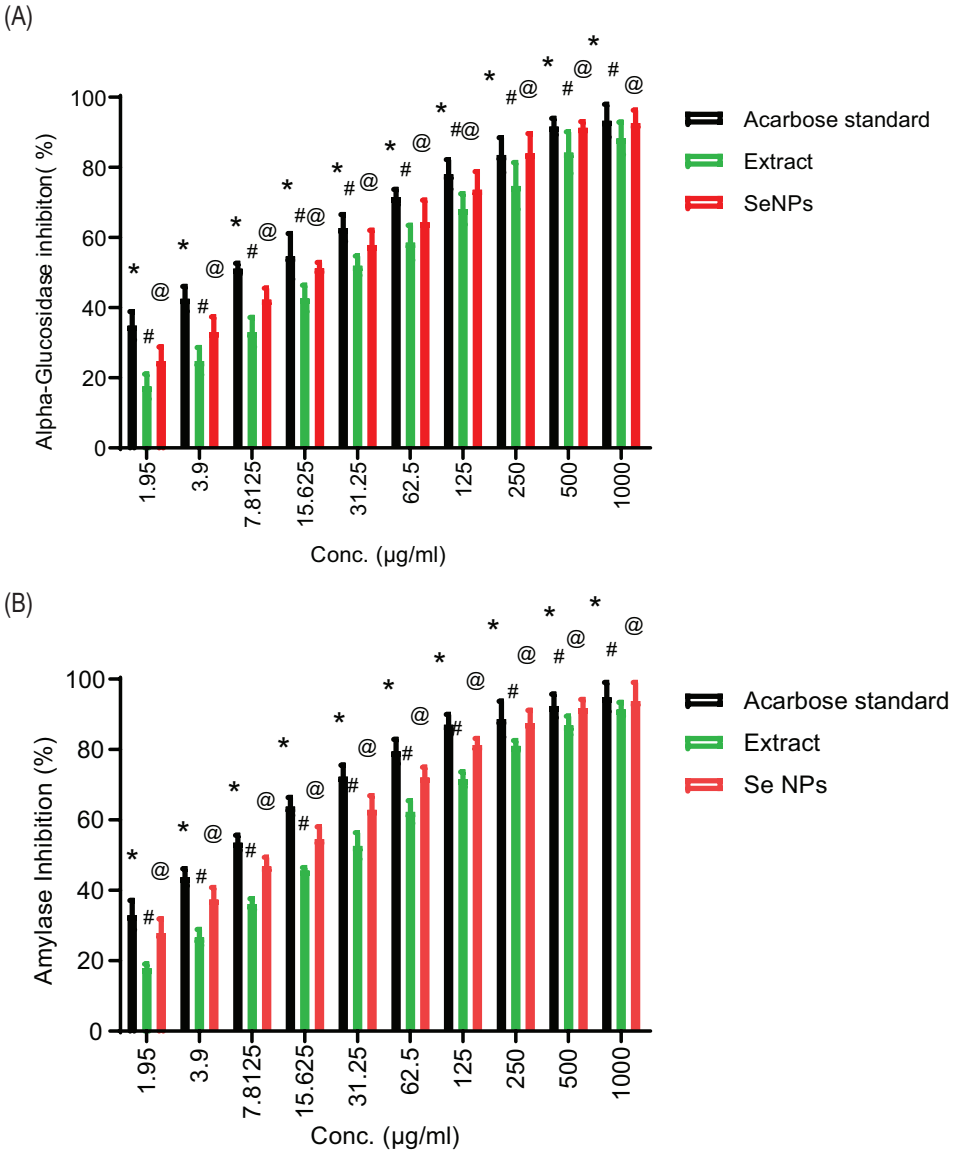

Figure 5. Antidiabetic activity of *S. costus* roots extract and SeNPs, compared to the control. The analysis was done by both (A) alpha glucosidase activity and (B) alpha amylase acarbose action (data are represented as mean±SD values; various symbols refer to significant variation at P ≤ 0.05).

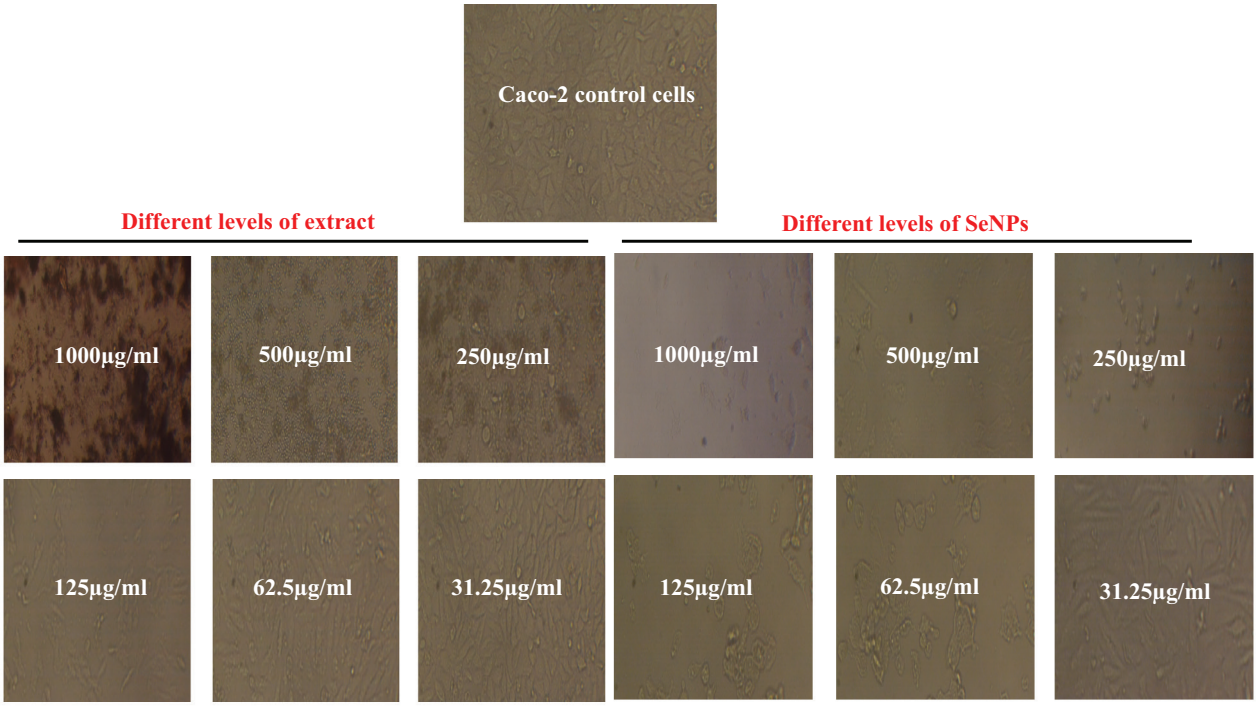

Figure 6. Microscopic examination of anticancer impact of various levels (1,000-31.25 µg/mL) of *S. costus* roots extract and SeNPs in two groups toward Caco-2 cells (magnification 40×).

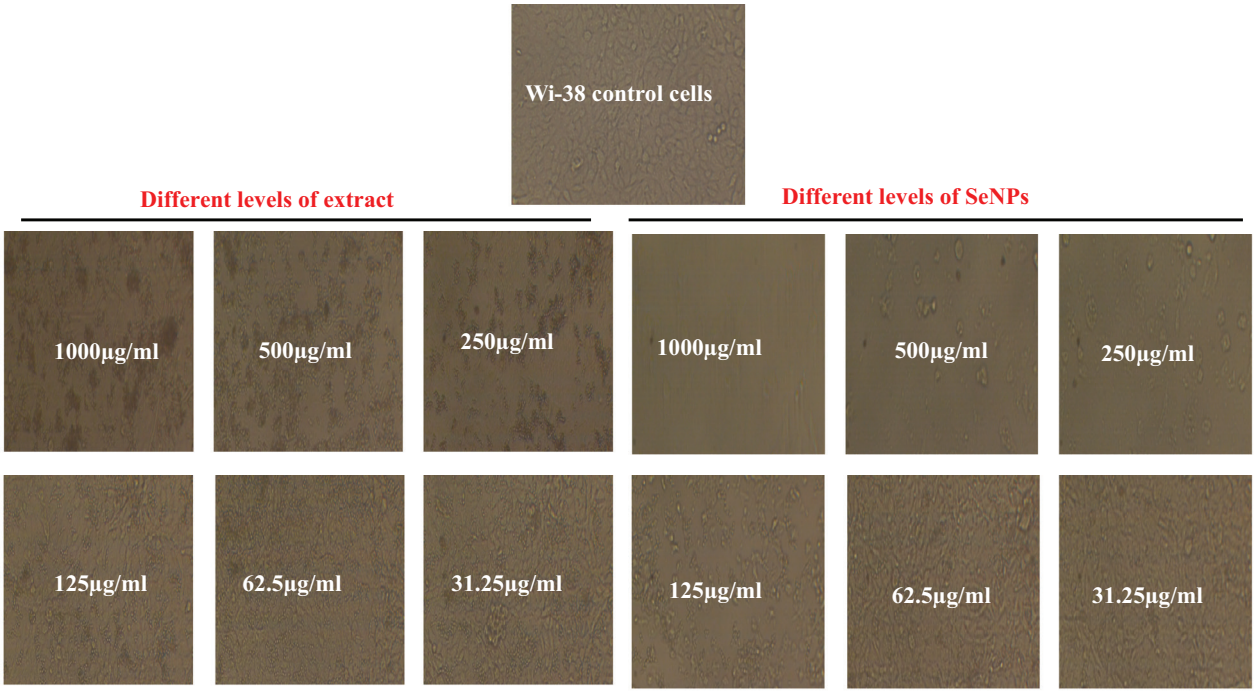

Figure 7. Microscopic examination of cytopathic impact of various levels (1,000-31.25 µg/mL) of *S. costus* roots extract and SeNPs in two groups toward Wi-38 cells (magnification 40×).

S and G1 phases upon using various treatments, compared to the control. In addition, there was a significant reduction in the proportion of M phase upon using *S. costus* extract ($P \leq 0.05$), compared to the control. The proportion of M phase reduced significantly upon using SeNPs ($P \leq 0.05$), compared to *S. costus* extract, revealing that SeNPs had the best anticancer impact (see Table 3 and Figure 8).

Different superscript letters in the same row reveal significant differences at $P \leq 0.05$.

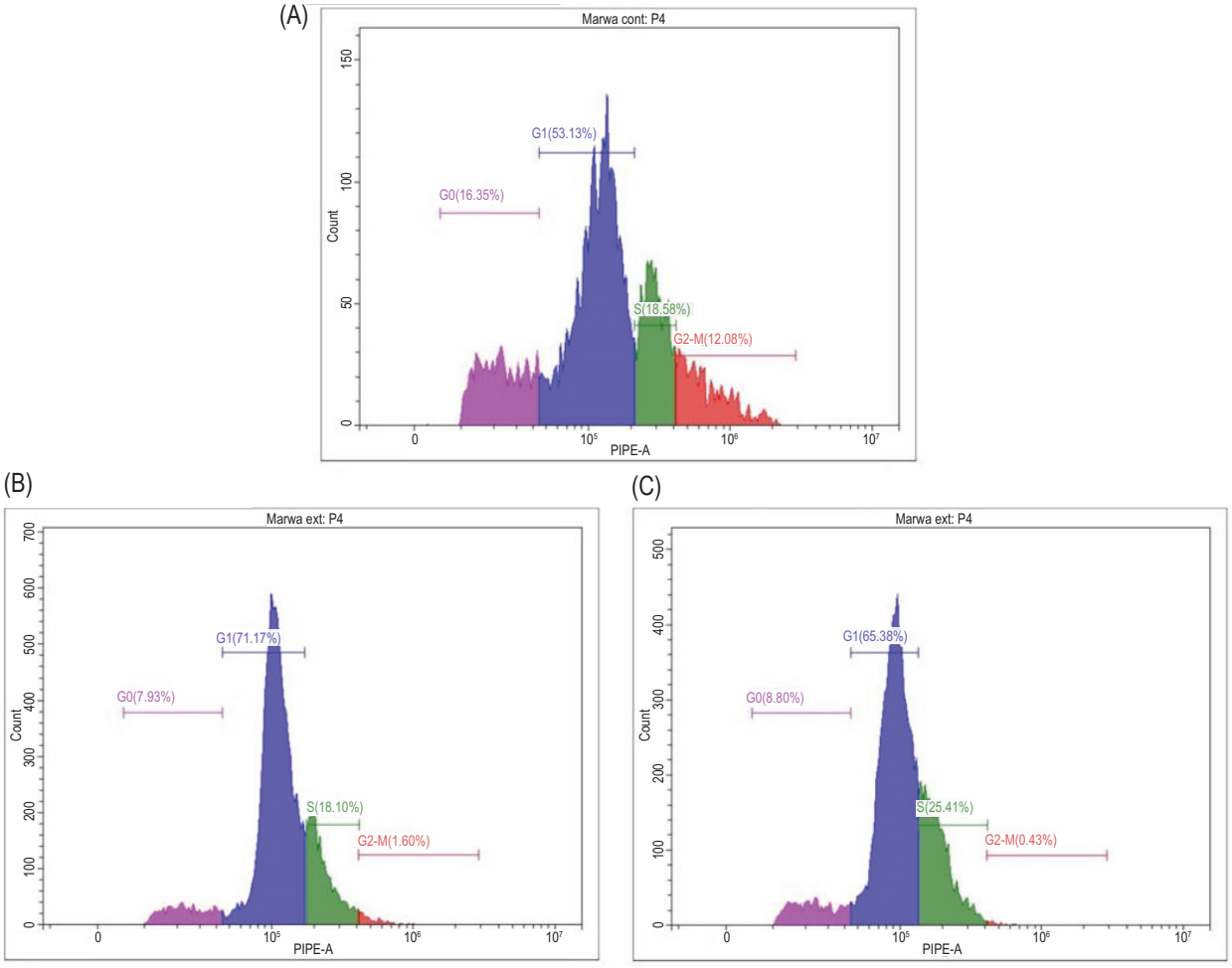

Figure 8. Flow cytometric analysis of different phases of cell cycle in (A) untreated Caco-2 cells, (B) treated Caco-2 cells by *S. costus* roots extract, and (C) treated Caco-2 cells by prepared SeNPs.

Table 3. Percentage distribution of Caco-2 cells in different cell-cycle phases after treatment with IC_{50} concentrations of *Saussurea costus* root extract and biosynthesized selenium nanoparticles (SeNPs), compared with untreated control cells.

Treatment phases	Control	*S. costus* extract	SeNPs
G0	16.3±0.1%[a]	7.93±0.1%[b]	8.80±0.1%[b]
S	18.58±0.2%[a]	18.10±0.3%[a]	25.41±0.4%[a]
G2-M	12.08±0.1%[a]	1.60±0.2%[b]	0.43±0.2%[c]
G1	53.13±0.2%[a]	71.17±0.1%[a]	65.38±0.1%[a]

Notes: Results are recorded as mean±SD values.

Discussion

Numerous studies have documented the application of plant chemicals to combat various bacterial infections (Kukić *et al.*, 2008). New and effective anticancer and antidiabetic medications with fewer adverse effects are also needed, and herbal remedies have shown promise as a source of these substances (DeSantis *et al.*, 2014). On the other hand, since selenium is an essential part of antioxidant enzymes and may play a crucial role in maintaining health, it has gained greater interest in recent years (Puri *et al.*, 2023). Traditional selenium substances are applied minimally because of their low safe dose level, which limits their applicability. However, materials at the nanometer scale exhibit physical and chemical properties that differ significantly from their bulk counterparts, enabling novel applications in various biomedical and technological fields. One such material is elemental selenium (Filipović *et al.*, 2021), while SeNPs are observed to be a more efficient and secure form of selenium with low adverse effects and high accessibility (AlBasher *et al.*, 2020).

In the present investigation, *S. costus* root extract showed a group of polyphenolic compounds and flavonoids upon HPLC testing, with rutin, chlorogenic acid, and coumaric acid being the most relevant compounds. Many studies showed that phenolic compounds could cause a variety of biological functions, and their ability of antioxidant effect was typically investigated in relation to their ability to eliminate free radicals' assessments (Singh *et al.*, 2016).

The TEM analysis revealed SeNPs as smooth and spherical particles with a relatively tiny shape, with an average diameter of 73.7±0.7 nm and a peak at 278 nm. Investigators had reported that the prepared SeNPs could have a size within a range of 50–400 nm, and changes in diameter could impact the stability and properties of nanoparticles (Mikhailova, 2023). Additionally, the presence of selenium in nano-solution, compared to *S. costus* extract, was demonstrated by FTIR, which displayed a distinctive peak at 462 cm^{-1} for SeNPs pattern. Decrease in the transmittance percentage of nearly all functional groups in FTIR showed strong evidence of the production of metal nanoparticles (Al-Brakati *et al.*, 2021). Other investigators used plant extracts to prepare metal nanoparticles (Abadi *et al.*, 2025; Mohammadi-Aghdam *et al.*, 2024).

The Gram -tive microaerobic bacterium *H. pylori* colonize in the stomach of humans causing chronic gastritis. Additionally, there is mounting evidence linking *H. pylori* infection to various illnesses, especially those involving mental, physiological, and cardiac processes (Pop *et al.*, 2022). Regarding the investigated substances' antibacterial activity, SeNPs demonstrated an anti-*H. pylori* effect with a MIC of 15.62±0.2 µg/mL and an inhibition diameter of 30.7±0.2 mm. Al-Saggaf *et al.* (2020) reported that selenium nanoparticles (SeNPs) synthesized using *Saussurea costus* extract exhibited anti-*Helicobacter pylori* activity, with a minimum inhibitory concentration (MIC) of 40 µg/mL.

The investigation and creation of antibacterial substances that can take the place of antibiotics in *H. pylori* medication has grown in popularity. Nanomaterials have attracted greater interest in health care because of their benefits, especially the superiority of metal-based nanoparticles over other nanoparticles (Yin *et al.*, 2023). Furthermore, Shirzadi-Ahodashti *et al.* (2021) reported the antibacterial activity of eco-friendly synthesized AgNPs against multi-drug-resistant bacteria.

The study's findings demonstrated that SeNPs' anti-inflammatory, antioxidant, antidiabetic, and anticancer properties outperformed those of *S. costus* extract. The elemental form of selenium is discovered to have a lower antioxidant property than its nanoform (Binsuwaidan *et al.*, 2024). Numerous investigations have demonstrated that SeNPs have more antioxidant capacity than the plant extract that was used to synthesize them (Bardaweel *et al.*, 2018; Barzegarparay *et al.*, 2024). Furthermore, studies showed the antioxidant level for *S. costus* at IC_{50} = 12.32 µg/mL (Mammate *et al.*, 2022), similar to the level discovered in the present work, that is 18.0±0.2 µg/mL. Thus, it was established that synthesized SeNPs could neutralize hydroxyl radicals. Since OH radicals make up the majority of reactive oxygen species (ROS), this is a crucial component. ROS can cause oxidative stress in living beings, an unbalance between the systemic generation of ROS and cells' capacity to immediately detoxify reactive intermediates or repair the resulting damage (Di Meo *et al.*, 2016). A new class of antioxidant therapeutics for the avoidance and management of oxidative stress-related disorders are nanoparticle antioxidants. They are stronger compared to the damage caused by free radicals, since they exhibit robust and long-lasting connections to structures (Sentkowska and Pyrzyńska, 2023). The data obtained validated SeNPs' excellent antioxidant activity.

The ability of a product to stabilize membranes suggests that it could be used to protect cell membranes, which are essential for numerous biological procedures (*Errasti-Murugarren et al., 2021*). Cell membranes are made up of proteins and lipids and serve a variety of purposes, including cellular signaling, transportation of waste and nutrients, and cell death (Zhai *et al.*, 2024). In the present study, both *S. costus* extract and the prepared SeNPs showed a promising anti-inflammatory impact, with SeNPs having a higher level of effect than *S. costus* extract. The present results revealed that SeNPs had an anti-inflammatory impact at IC50 = 8.33±0.4 µg/mL. On the other hand Almayouf *et al.* (2024) reported a DPPH value for AgNPS prepared from *S. costus* extract at IC_{50} = 120 µg/mL.

Diabetes mellitus is a common endocrine condition that ranks as the fourth most common cause of death worldwide. This ailment has not yet been satisfactorily cured by allopathic medication. Innovative antidiabetic strategies with improved management and fewer adverse effects and less expenses are therefore desperately needed (Ahmed *et al.*, 2017). The present study highlights the antidiabetic effect of SeNPs, which was higher than that of *S. costus* extract, similar to the results showed by Ahmed *et al.* (2017) and Karas *et al.* (2024)

Conclusion

The current research reports on the anti-*H. pylori* activity of SeNPs obtained from the root extract of *S. costus*. The findings showed that SeNPs had strong anti-inflammatory and antioxidant effects. They showed a promising antidiabetic effect that was corroborated by alpha glucosidase and alpha amylase activity. SeNPs showed substantial anticancer effects toward Caco-2 cells, confirmed by enhancing early apoptosis in cell cycle. Overall, the biosynthesized SeNPs demonstrated strong antioxidant, anti-inflammatory, antidiabetic, and anticancer activities, with minimal cytotoxicity toward normal cells. These findings suggest their potential for

safe therapeutic use; however, further in vivo animal studies are required to confirm their safety and efficacy before large-scale or clinical application

Data Availability Statement

All data generated in this work are available with the author upon reasonable request.

Author Contributions

M.A. (Manal Almughamisi) performed all aspects of the research and preparation of the manuscript and has read and approved the published version.

Conflicts of Interest

The author declared no conflict of interest.

Funding

This research received no specific grant from any funding agency in the public, commercial, or not-for-profit sectors.

References

Abadi, E.H.L., Amiri, M., Ranaee, M., Mortazavi-Derazkola, S., Khademian, A., Najafzadehvarzi, H. and Ghoreishi, S.M. 2025. Plasmonic selenium nanoparticles biosynthesized from *Crataegus monogyna* fruit extract: a novel approach to mitigating chromium-induced toxicity. Plasmonics 20: 3805–3815. https://doi.org/10.1007/s11468-024-02539-3

Adibian, F., Ghaderi, R.S., Sabouri, Z., Davoodi, J., Kazemi, M., Ghazvini, K., Youssefi, M., Soleimanpour, S. and Darroudi, M. 2022. Green synthesis of selenium nanoparticles using *Rosmarinus officinalis* and investigated their antimicrobial activity. Biometals 35(1): 147–158. https://doi.org/10.1007/s10534-021-00356-3

Ahmed, H.H., Abd El-Maksoud, M.D., Abdel Moneim, A.E. and Aglan, H.A. 2017. Pre-clinical study for the antidiabetic potential of selenium nanoparticles. Biological Trace Element Research 177(2): 267–280. https://doi.org/10.1007/s12011-016-0876-z

Ahmed, H.Y., Kareem, S.M., Atef, A., Safwat, N.A., Shehata, R.M., Yosri, M., Youssef, M., Baakdah, M.M., Sami, R., Baty, R.S., Alsubhi, N.H., Alrefaei, G.I., Shati, A.A. and Elsaid, F.G. 2022. Optimization of supercritical carbon dioxide extraction of *Saussurea costus* oil and its antimicrobial, antioxidant, and anticancer activities. Antioxidants (Basel) 11(10): 1960. https://doi.org/10.3390/antiox11101960

AlBasher, G., Alfarraj, S., Alarifi, S., Alkhtani, S., Almeer, R., Alsultan, N., Alharthi, M., Alotibi, N., Al-bass, A. and Abdel Moneim, A.E. 2020. Nephroprotective role of selenium nanoparticles against glycerol-induced acute kidney injury in rats. Biological Trace Element Research 194: 444–454.

Al-Brakati, A., Alsharif, K.F., Alzahrani, K.J., Kabrah, S., Al-Amer, O., Oyouni, A.A., Habotta, O.A., Lokman, M.S., Bauomy, A.A., Kassab, R.B., et al. 2021. Using green biosynthesized lycopene-coated selenium nanoparticles to rescue renal damage in glycerol-induced acute kidney injury in rats. International Journal of Nanomedicine 16: 4335–4349.

Alduais, M.A., El Rabey, H.A., Mohammed, G.M., Al-Awthan, Y.S., Althiyabi, A.S., Attia, E.S., Rezk, S.M. and Tayel, A.A. 2025. The anticancer activity of fucoidan coated selenium nanoparticles and curcumin nanoparticles against colorectal cancer lines. Scientific Reports 15(1): 287. https://doi.org/10.1038/s41598-024-82687-y

Almayouf, M.A., Charguia, R., Awad, M.A., Ben Bacha, A. and Ben Abdelmalek, I. 2024. Nanotherapy for cancer and biological activities of green synthesized AgNPs using aqueous *Saussurea costus* leaves and roots extracts. Pharmaceuticals (Basel). 17(10): 1371. https://doi.org/10.3390/ph17101371

Alsanosi, S., Sheikh, R.A., Sonbul, S., Altayb, H.N., Batubara, A.S., Hosawi, S., Al-Sakkaf, K., Abdullah, O., Omran, Z. and Alhosin, M. 2022. The potential role of *Nigella sativa* seed oil as epigenetic therapy of cancer. Molecules 27: 2779. https://doi.org/10.3390/molecules27092779

Alshahrani, S.H., Alameri, A.A., Zabibah, R.S., Jalil, A.T.J., Ahmadi, O. and Behbudi, G. 2022. Screening method synthesis of AgNPs using *Petroselinum crispum* (parsley) leaf: spectral analysis of the particles and antibacterial study. Journal of the Mexican Chemical Society 66(4),480-487: https://doi.org/10.29356/jmcs.v66i4.1803

Amina, M., Arumugham, M.I., Ramalingam, K. and Rajeshkumar, S. 2023. Evaluation of the anti-inflammatory, antimicrobial, antioxidant, and cytotoxic effects of chitosan thiocolchicoside-lauric acid nanogel. Cureus. 15(9): e46003. https://doi.org/10.7759/cureus.46003

Ao, B., Du, Q., Liu, D., Shi, X., Tu, J. and Xia, X. 2023. A review on synthesis and antibacterial potential of bio-selenium nanoparticles in the food industry. Frontiers in Microbiology 14: 1229838. https://doi.org/10.3389/fmicb.2023.1229838

Azmir, J., Zaidul, I.S.M., Rahman, M.M., Sharif, K.M., Mohamed, A., Sahena, F., Jahurul, M.H.A., Ghafoor, K., Norulaini, N.A.N. and Omar, A.K.M. 2013. Techniques for extraction of bioactive compounds from plant materials: a review. Journal of Food Engineering (JFE) 117: 426–436. https://doi.org/10.1016/j.jfoodeng.2013.01.014

Bardaweel, S.K., Gul, M., Alzweiri, M., Ishaqat, A., ALSalamat, H.A. and Bashatwah, R.M. 2018. Reactive oxygen species: the dual role in physiological and pathological conditions of the human body. Eurasian Journal of Medicine 50: 93–201.

Barzegarparay, F., Najafzadehvarzi, H., Pourbagher, R., Parsian, H., Ghoreishi S.M. and Mortazavi-Derazkola, S. 2024. Green synthesis of novel selenium nanoparticles using *Crataegus monogyna* extract (SeNPs@CM) and investigation of its toxicity, antioxidant capacity, and anticancer activity against MCF-7 as a breast cancer cell line. Biomass Conversion

& Biorefinery 14: 25369–25378. https://doi.org/10.1007/s13399-023-04604-z

Bhattacharya, D. and Rajinder, G. 2005. Nanotechnology and potential of microorganisms. Critical Reviews in Biotechnology 25: 199–204. https://doi.org/10.1080/07388550500361994

Binsuwaidan, R., El-Masry, T.A., El-Nagar, M.M.F., El Zahaby E.I., Gaballa, M.M.S. and El-Bouseary, M.M. 2024. Investigating the antibacterial, antioxidant, and anti-inflammatory properties of a lycopene selenium nano-formulation: an *in vitro* and *in vivo* study. Pharmaceuticals (Basel) 17(12): 1600. https://doi.org/10.3390/ph17121600

Cháirez-Ramírez, M.H., de la Cruz-López, K.G. and García-Carrancá, A. 2021. Polyphenols as antitumor agents targeting key players in cancer-driving signaling pathways. Frontiers in Pharmacology 12: 710304. https://doi.org/10.3389/fphar.2021.710304

DeSantis, C.E., Lin, C.C., Mariotto, A.B., Siegel, R.L., Stein, K.D. and Kramer, J.L. 2014. Cancer treatment and survivor ship statistics. CA Cancer Journal for Clinicians 64: 252–271. https://doi.org/10.3322/caac.21235

Di Meo, S., Reed, T.T., Venditti, P. and Victor, V.M. 2016. Role of ROS and RNS sources in physiological and pathological conditions. Oxidative Medicine and Cellular Longevity 2016: 1245049.

Elnour, A.A.M. and Abdurahman, N.H. 2024. Current and potential future biological uses of *Saussurea costus* (Falc.) Lipsch: a comprehensive review. Heliyon 10(18): e37790. https://doi.org/10.1016/j.heliyon. 2024.e37790

Elshaer, S.E., Hamad, G.M., Hafez, E.E., Baghdadi, H.H., El-Demerdash, F.M. and Simal-Gandara, J. 2022. Root extracts of *Saussurea costus* as prospective detoxifying food additive against sodium nitrite toxicity in male rats. Food and Chemical Toxicology 166: 113225. https://doi.org/10.1016/j.fct.2022.113225

Elshaer, S.E., Hamad, G.M., Sobhy, S.E., Darwish, A.M.G., Baghdadi, H.H., Abo Nahas, H., El-Demerdash, F.M., Kabeil, S.S.A., Altamimi, A.S., Al-Olayan, E., Alsunbul, M., Docmac, O.K., Jaremko, M., Hafez, E.E. and Saied, E.M. 2024. Supplementation of *Saussurea costus* root alleviates sodium nitrite-induced hepatorenal toxicity by modulating metabolic profile, inflammation, and apoptosis. Frontiers in Pharmacology 15: 1378249. https://doi.org/10.3389/fphar.2024.1378249

Errasti-Murugarren, E., Bartoccioni, P. and Palacín, M. 2021. Membrane protein stabilization strategies for structural and functional studies. Membranes (Basel) 11(2): 1–17. https://doi.org/10.3390/membranes11020155

Esmaili, S., Zinsaz, P., Ahmadi, O, Najian, Y., Vaghari, H. and Jafarizadeh-Malmiri, H. 2022. Screening of four accelerated synthesized techniques in green fabrication of ZnO nanoparticles using Willow *leaf extrac*t. Zeitschrift für Physikalische Chemie, 236 (11-12), 1567-1581), https://doi.org/10.1515/zpch-2022-0036

Filipović, N., Ušjak, D., Milenković, M.T., Zheng, K., Liverani, L., Boccaccini, A.R. and Stevanović, M.M. 2021. Comparative study of the antimicrobial activity of selenium nanoparticles with different surface chemistry and structure. Frontiers in Bioengineering and Biotechnology 8: 624621.

Garza-García, J.J.O., Hernández-Díaz, J.A., León-Morales, J.M. et al. 2023. Selenium nanoparticles based on *Amphipterygium glaucum* extract with antibacterial, antioxidant, and plant biostimulant properties. Journal of Nanobiotechnology 21: 252. https://doi.org/10.1186/s12951-023-02027-6

Ghoreishi, S.M. and Mortazavi-Derazkola, S. 2025. Eco-friendly synthesis of gold nanoparticles via tangerine peel extract: unveiling their multifaceted biological and catalytic potentials. Heliyon 11(1): e40104.

Gueffai, A., Gonzalez-Serrano, D.J., Christodoulou, M.C., Orellana-Palacios, J.C., Ortega, M.L.S., Ouldmoumna, A., Kiari, F.Z., Ioannou, G.D., Kapnissi-Christodoulou, C.P., Moreno, A. and Hadidi, M. 2022. Phenolics from defatted black cumin seeds (*Nigella sativa* L.): ultrasound-assisted extraction optimization, comparison, and antioxidant activity. Biomolecules 12(9): 1311. https://doi.org/10.3390/biom12091311

Gupta, A., Behl, T., Singh, S., Garg, M., Tamboli, E.T., Chigurupati, S., Felemban, S.G., Albarrati, A., Albratty, M. and Meraya, A.M. 2023. Quantification of luteolin, apigenin and chrysoeriol in *Tecoma stans* by RP-HPLC method. Journal of Chromatographic Science 61(9): 844–851. https://doi.org/10.1093/chromsci/bmad022

Hashemi, Z., Zirar M. Mizwari, Z.M., Alizadeh, S.R., Habibi, M., Rezaee, S.M., Ghoreishi, S.M., Mortazavi-Derazkola, S. and Ebrahimzadeh, M.A. 2023. Anticancer and antibacterial activity against clinical pathogenic multi-drug-resistant bacteria using biosynthesized silver nanoparticles with *Mentha pulegium* and *Crocus caspius* extracts. Inorganic Chemistry Communications 154: 110982. https://doi.org/10.1016/j.inoche.2023.110982

Huang, X., Liu, Y., Lin, Z., Wu, B., Nong, G., Chen, Y., Lu, Y., Ji, X., Zhou, X., Suo, B., Chen, Q. and Wei, J. 2021. Minimum inhibitory concentrations of commonly used antibiotics against Helicobacter pylori: a multicenter study in South China. PLoS One 16(9): e0256225. https://doi.org/10.1371/journal.pone.0256225

Karas, R.A., Alexeree, S., Elzohery, N. et al. 2024. Antidiabetic potential of selenium nanoparticles and plasma-rich platelets in diabetic mice. Applied Biological Chemistry 67: 62. https://doi.org/10.1186/s13765-024-00907-5

Karim, N., Liu, S., Rashwan, A.K., Xie J., Mo, J., Osman, A.I., Rooney, D.W. and Chen, W. 2023. Green synthesis of nanolipo-fbersomes using Nutriose® FB 06 for delphinidin-3-O-sambubioside delivery: characterization, physicochemical properties, and application. International Journal of Biological Macromolecules 247: 125839. https://doi.org/10.1016/j.ijbiomac.2023.125839

Kibria, M.R., Akbar, R.I., Nidadavolu, P., Havryliuk, O., Lafond, S. and Azimi, S. 2023. Predicting efficacy of drug-carrier nanoparticle designs for cancer treatment: a machine learning-based solution. Scientific Reports 13(1): 547. https://doi.org/10.1038/s41598-023-27729-7

Korde, P., Ghotekar, S., Pagar, T., Pansambal, S., Oza, R. and Mane, D. 2020. Plant extract-assisted eco-benevolent synthesis of selenium nanoparticles—a review on plant parts involved, characterization and their recent applications. Journal of Chemical Reviews 2(3): 157–168.

Kukić, J., Popović, V., Petrović, S., Mucaji, P., Ćiric, A. and Stojković, D. 2008. Antioxidant and antimicrobial activity of *Cynara cardunculus* extracts. Food Chemistry 107: 861–868. https://doi.org/10.1016/j.foodchem.2007.09.005

Mammate N., El Oumari F.E., Imtara H., Belchkar S., Lahrichi A., Alqahtani A.S., Noman O.M., Tarayrah M. and Houssaini T.S. 2022. Antioxidant and anti-urolithiatic activity of aqueous and ethanolic extracts from *Saussurea costus* (Falc) lispich using scanning electron microscopy. Life (Basel) 12(7): 1026. https://doi.org/10.3390/life12071026

Marinova, D.F., Ribarova, F. and Atanassova, M. 2005. Total phenolic and total flavonoids in Ulgarian fruits and vegetables. Journal of the University of Chemical Technology and Metallurgy 40(3): 255–260.

Mellinas, C., Jiménez, A. and Garrigós, M.D.C. 2019. Microwave-assisted green synthesis and antioxidant activity of selenium nanoparticles using *Theobroma cacao* L. bean shell extract. Molecules 24(22): 40–48. https://doi.org/10.3390/molecules24224048

Mikhailova E.O. Selenium nanoparticles: green synthesis and biomedical application. Molecules 28(24): 8125. https://doi.org/10.3390/molecules28248125

Mohammadi-Aghdam, S., Bahraini, F. and Ghoreishi, S.M. 2024. *In vitro* anticancer on acute lymphoblastic leukemia NALM-6 cell line, antibacterial and catalytic performance of eco-friendly synthesized ZnO and Ag-doped ZnO nanoparticles using Hedera colchica extract. Biomass Conversion and Biorefinery 14: 20037–20052. https://doi.org/10.1007/s13399-023-04562-6

Mohanpuria, P., Rana, N.K. and Yadav S.K. 2008. Biosynthesis of nanoparticles: technological concepts and future applications. Journal of Nanoparticle Research 10: 507–517. https://doi.org/10.1007/s11051-007-9275-x

Mujammami, M. 2020. Clinical significance of *Saussurea costus* in thyroid treatment. Saudi Medicine Journal 41(10): 1047–1053. https://doi.org/10.15537/smj.2020.10.25416

Oboh, G., Akinyemi, A.J. and Ademiluyi, A.O. 2012. Inhibition of α-amylase and α-glucosidase activities by ethanolic extract of *Telfairia occidentalis* (fluted pumpkin) leaf. Asian Pacific Journal of Tropical Biomedicine 2(9): 733–738. https://doi.org/10.1016/S2221-1691(12)60219-6

Othman, M.S., Obeidat, S.T., Al-Bagawi, A.H., Fareid, M.A., Fehaid, A. and Abdel Moneim, A.E. 2022. Green-synthetized selenium nanoparticles using berberine as a promising anticancer agent. Journal of Integrated Medicine 20(1): 65–72. https://doi.org/10.1016/j.joim.2021.11.002

Pon Matheswari, P., Jenit Sharmila, G. and Murugan, C. 2022. Green synthesis of selenium nanoparticles using *Delonix regia* and *Nerium oleander* flower extract and evaluation of their antioxidant and antibacterial activities. Inorg and Nano-Met Chemistry 54(5): 1–12. https://doi.org/10.1080/24701556.2021.2025099

Pop, R., Tăbăran, A.F., Ungur, A.P., Negoescu, A. and Cătoi, C. 2022. *Helicobacter pylori*-induced gastric infections: from pathogenesis to novel therapeutic approaches using silver nanoparticles. Pharmaceutics 14(7): 1463. https://doi.org/10.3390/pharmaceutics14071463

Puri, A., Mohite, P., Patil, S., Chidrawar, V.R., Ushir, Y.V., Dodiya, R. and Singh, S. 2023. Facile green synthesis and characterization of *Terminalia arjuna* bark phenolic-selenium nanogel: a biocompatible and green nano-biomaterial for multifaceted biological applications. Frontiers in Chemistry 11: 1273360.

Rezaei, A., Morsali, A., Bozorgmehr, M.R. and Nasrabadi, M. 2021. Quantum chemical analysis of 5-aminolevulinic acid anticancer drug delivery systems: carbon nanotube, –COOH functionalized carbon nanotube and iron oxide nanoparticle. Journal of Molecular Liquids 340: 117182. https://doi.org/10.1016/j.molliq.2021.117182

Santiago, M.B., Leandro, L.F., Rosa, R.B., Silva, M.V., Teixeira, S.C., Servato, J.P.S., Ambrósio, S.R., Veneziani, R.C.S., Aldana-Mejía, J.A., Bastos, J.K. and Martins, C.H.G. 2022. Brazilian red propolis presents promising anti-*H. pylori* activity in *in vitro* and *in vivo* assays with the ability to modulate the immune response. Molecules 27(21): 7310. https://doi.org/10.3390/molecules27217310

Sastry, M., Ahmad, A., Khan, M.I. and Kumar, R. 2004. Microbial nanoparticle production. In: Niemeyer C.M. and Mirkin C.A. (eds.) Nanobiotechnology. Wiley-VCH, Weinheim, Germany, pp. 126–135.

Sentkowska, A. and Pyrzyńska, K. 2023. Antioxidant properties of selenium nanoparticles synthesized using tea and herb water extracts. Applied Sciences 13*:* 1071. https://doi.org/10.3390/app13021071

Shayan, S., Hajihajikolai, D., Ghazale, F., Gharahdaghigharahtappeh, F., Faghih, A., Ahmadi, O. and Behbudi, G. 2024. Optimization of green synthesis formulation of selenium nanoparticles (SeNPs) using peach tree leaf extract and investigating its properties and stability. Iranian Journal of Biotechnology 22(3): e3786. https://doi.org/10.30498/ijb.2024.413943.3786

Shirzadi-Ahodashti, M., Mizwari, Z.M., Hashemi, Z., Rajabalipour, Masoumeh, S.S., Ghoreishi, M., Mortazavi-Derazkola, S. and Ali Ebrahimzadeh, M.A. 2021. Discovery of high antibacterial and catalytic activities of biosynthesized silver nanoparticles using *C. fruticosus* (CF-AgNPs) against multi-drug resistant clinical strains and hazardous pollutants. Environmental Technology & Innovation 23: 101607. https://doi.org/10.1016/j.eti.2021.101607

Singh, G., Passsari, A.K., Leo, V.V., Mishra, V.K., Subbarayan, S., Singh, B.P., Kumar, B., Kumar, S., Gupta, V.K., Lalhlenmawia, H. and Nachimuthu, S.K. 2016. Evaluation of phenolic content variability along with antioxidant, antimicrobial, and cytotoxic potential of selected traditional medicinal plants from India. Frontiers in Plant Science 7: 407. https://doi.org/10.3389/fpls.2016.00407

Soliman, M.K., Amin, M.A.A., Nowwar, A.I. et al. 2024. Green synthesis of selenium nanoparticles from *Cassia javanica* flowers extract and their medical and agricultural applications. Scientific Reports 14: 26775. https://doi.org/10.1038/s41598-024-77353-2

Taher, M.A.H., Dawood, D.H., Sanad, M.I. and Hassan, R.A. 2026. Searching for anti-hyperglycemic phytomolecules of Tecoma stans. European Journal of Chemistry 7(4): 397–404. https://doi.org/10.5155/eurjchem.7.4.397-404.1478

Tsiaka, T., Sinanoglou, V.J. and Zoumpoulakis, P. 2017. Extracting bioactive compounds from natural sources using green high-energy approaches: trends and opportunities in lab- and large-scale applications. In:A.M.Grumezescu and A.M.Holban (Eds.), *Ingredients Extraction by Physicochemical Methods in Food*, pp. 307–365. Academic Press, Cambridge, MA.

Xu, Y., Rashwan, A.K., Osman, A.I., Abd El-Monaem, E.M., Elgarahy, A.M., Eltaweil, A.S., Omar, M., Li, Y., Mehanni, A.-H.E., Chen, W., et al. 2023. Synthesis and potential applications of cyclodextrin based metal-organic frameworks: a review. Environmental Chemistry Letters 21: 447–477. https://doi.org/10.1007/s10311-022-01509-7

Yin, X., Lai, Y., Du, Y., Zhang, T., Gao, J. and Li, Z. 2023. Metal-based nanoparticles: a prospective strategy for *Helicobacter pylori* treatment. International Journal of Nanomedicine 18: 2413–2429. https://doi.org/10.2147/IJN.S405

Zhai, Y., Peng, W., Luo, W., Wu, J., Liu, Y and Wang F. 2024. Component stabilizing mechanism of membrane-separated hydrolysates on frozen surimi. Food Chemistry 431: 137114.

Supplementary

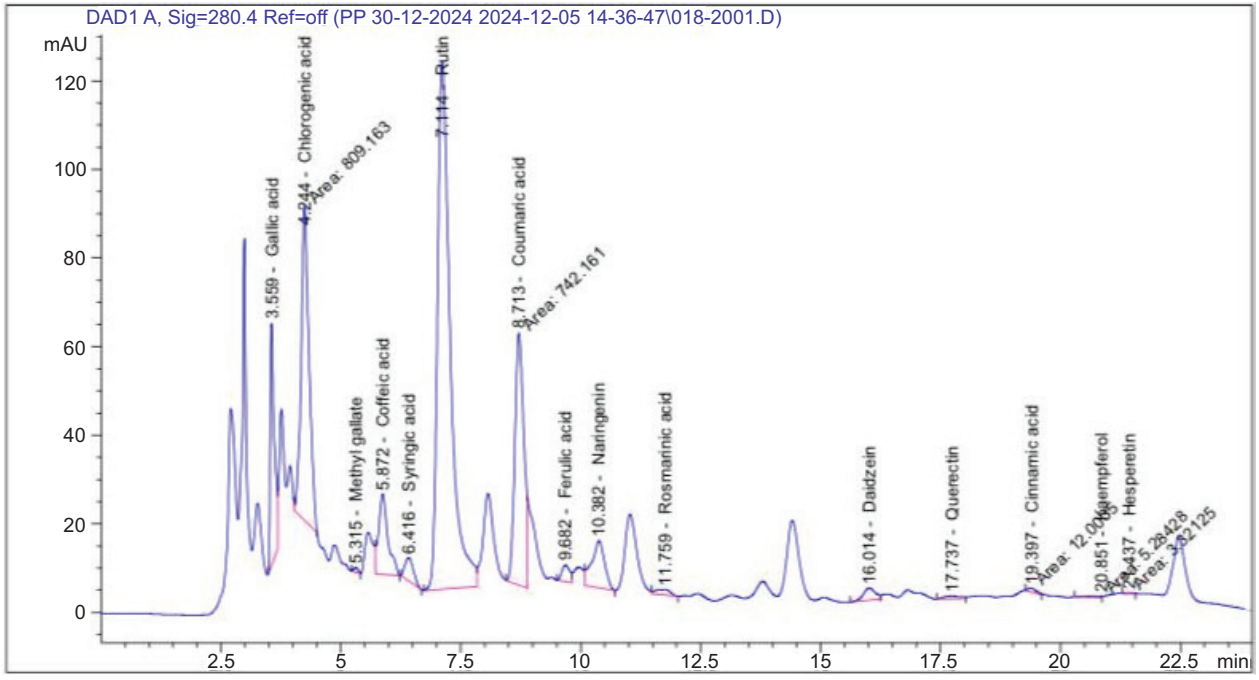

Figure S1. HPLC chromatogram for the of ethanol extract of S. costus roots.

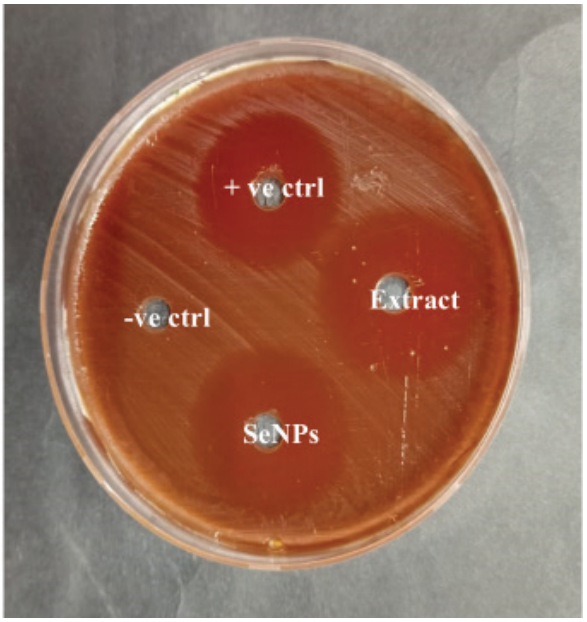

Figure S2. Examination of antibacterial activity toward *H. pylori*. (Notes: -ve ctrl: negative control; +ve ctrl: positive control; Extract: *S. costus* roots extract; SeNPs: selenium nanoparticles.)

Table S1. Detection of anticancer impact of *S. costus* extract and the prepared SeNPs tested at serial concentration ranging from (31.25 to 1000 µg/mL) toward Caco-2 cells.

ID	µg/mL	OD			Mean OD	±SE	Viability (%)	Toxicity (%)	IC_{50}±SD
Caco-2	--------	0.704	0.709	0.696	0.703	0.003786	100	0	µg
S. costus extract	1,000	0.043	0.044	0.044	0.043667	0.000333	6.211474633	93.78852537	82.77±1.02
	500	0.057	0.05	0.062	0.056333	0.00348	8.013276434	91.98672357	
	250	0.075	0.063	0.069	0.069	0.003464	9.815078236	90.18492176	
	125	0.148	0.134	0.156	0.146	0.006429	20.76813656	79.23186344	
	62.5	0.397	0.382	0.377	0.385333	0.006009	54.81270744	45.18729256	
	31.25	0.701	0.704	0.702	0.702333	0.000882	99.90516833	0.094831674	
SeNPs	1,000	0.022	0.019	0.02	0.020333	0.000882	2.89236605	97.10763395	34.09±2.49
	500	0.021	0.02	0.02	0.020333	0.000333	2.89236605	97.10763395	
	250	0.027	0.03	0.028	0.028333	0.000882	4.030346136	95.96965386	
	125	0.064	0.059	0.071	0.064667	0.00348	9.198672357	90.80132764	
	62.5	0.099	0.084	0.091	0.091333	0.004333	12.99193931	87.00806069	
	31.25	0.365	0.379	0.384	0.376	0.005686	53.48506401	46.51493599	

Note: Results are presented as mean±SD values.

Table S2. Detection of toxic impact of *S. costus* extract and the prepared SeNPs tested at serial concentration various levels ranging from (31.25 to 1000 µg/mL) toward Wi-38 cells.

ID	µg/mL	OD			Mean OD	±SE	Viability (%)	Toxicity (%)	IC_{50}±SD
Wi38	--------	0.741	0.746	0.748	0.745	0.002082	100	0	µg/mL
S. costus extract	1,000	0.035	0.044	0.043	0.040667	0.002848	5.458612975	94.54138702	146.5±0.52
	500	0.047	0.04	0.044	0.043667	0.002028	5.861297539	94.13870246	
	250	0.048	0.05	0.057	0.051667	0.002728	6.935123043	93.06487696	
	125	0.345	0.355	0.36	0.353333	0.00441	47.42729306	52.57270694	
	62.5	0.721	0.718	0.72	0.719667	0.000882	96.59955257	3.400447427	
	31.25	0.746	0.74	0.743	0.743	0.001732	99.73154362	0.268456376	
Se NPs	1,000	0.022	0.02	0.024	0.022	0.001155	2.953020134	97.04697987	87.91±0.45
	500	0.027	0.023	0.031	0.027	0.002309	3.624161074	96.37583893	
	250	0.046	0.052	0.046	0.048	0.002	6.44295302	93.55704698	
	125	0.116	0.132	0.126	0.124667	0.004667	16.73378076	83.26621924	
	62.5	0.573	0.577	0.563	0.571	0.004163	76.6442953	23.3557047	
	31.25	0.717	0.708	0.712	0.712333	0.002603	95.61521253	4.384787472	

Note: Results are presented as mean±SD values.